Morphological Engineering of Porphyrin Porous Organic Polymers

Mingxuan Li

College of Materials Science and Engineering, Beijing University of Chemical Technology, Beijing 100029, China
Email: 2019020413@mail.buct.edu.cn
Manuscript received January 20, 2023; revised March 30, 2023; accepted May 25, 2023; published June 13, 2024

***Abstract*—Porphyrin Porous Organic Polymers (POPs) have been proved to have outstanding photocatalytic activity and can be used in several fields. Our research aims to the morphological engineering of porphyrin POPs materials. Using SiO_2 as template materials, the morphological structures of Porphyrin POPs could be well controlled in the nanoscale. We modified the silica sphere with amino group and aldehyde group and then used the typical Stöber method to synthesize the porphyrin structure. The samples were well characterized by nitrogen adsorption, Power X-Ray Diffraction (PXRD), Transmission Electron Microscopy (TEM) and Fourier-Transform Infrared Spectroscopy (FTIR) spectra and the analysis results showed that the morphorlogy and size of the sphere Porphyrin POPs were well controlled. After etch, we get a shell structure made by polyporphyrin POPs in nanoscale. The shell structure of the porphyrin POPs paving the way for the applications as treatment platform in vivo.**

***Keywords*—morphological engineering, template method, porphyrin, porous organic polymers**

I. Introduction

Porphyrin Porous Organic Polymers (POPs) shows a great catalytic activity and photodynamic activity because of its unique structure. Combing with the porphyrin building block and porous structure, porphyrin POPs could be used in Photothermal Therapy (PTT) and Photodynamic Therapy (PDT) agents to treat cancer. Photothermal Therapy (PTT) and Photodynamic Therapy (PDT) was considered as effective individual or coupling treatments for cancer, as these two methods show higher accuracy and better therapeutic effect in comparison with traditional treatments, such as surgery and chemotherapeutics [1]. During the photochemical reaction, porphyrin structure can transform the energy of the light to produce heat or active free Radicals like Oxygen Species (ROS) especially singlet oxygen ($^1O_2$), to break the protein, the lipid and DNA of tumor cells and result in cell death [2, 3]. During the process, the porous structure and high surface area of the porphyrin POPs will accelerate the produce and transfer of the heat and oxygen species. POPs can play a significant role in developing the novel nano-platform based on porphyrin POPs for PTT and PDT therapy.

The performance of porphyrin POPs as nano-platform for PTT and PDT therapy is critically dependent on the morphological structures. As we know, the size of a nanoparticle is the essential parameter for effective delivery and cell permeability. The enhanced permeability and retention effect, that the gap in tumor issues (50~200 nm) is wider than normal tissues' gap (<50 nm), resulting in the selectivity and hysteresis of macromolecule and nanoparticles with suitable size [4]. For the application in vivo as a platform for cancer therapy, the porphyrin POPs with bulk morphology in nature need morphological engineering for a nano size. In addition, morphological engineering improves the performance of POPs by control the volume and size of particles [5]. For example, Zheng's group used self-template method to synthesize shell POP nanoparticles and showed an outstanding morphological structure and a better cancer treatment performance [6]. Besides, the hollow structure of POPs demonstrates a good prospect to load hydrophobic drug and extended its function to the field of chemotherapeutics.

In this work, a well-defined Hollow porphyrin based Porous Organic Polymers (H-POP) was fabricated using hard template method as presented in Fig. 1. Employed SiO_2 nanoparticle as the template, nano porphyrin POPs shell was synthesized through a facile bottom-up approach by using extended aromatic substitution reaction of pyrrole with 4,4-diformyl-1,1'-biphenyl, in which the complex preparation procedure of monomer was avoided [7]. By miniaturization H-POP to nanoscale, the water-dispersibility and cell permeability of H-POP will be improved, and the PDT and PTT performance will be evaluated in further study.

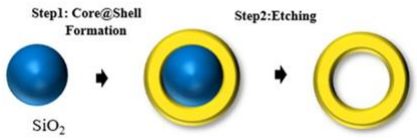

Fig. 1. Schematic diagram of synthesis of H-POP.

II. Experimental Section

A. Reagents

The following materials were used in our experiments: Ethanol, ammonium hydroxide, Tetraethyl Orthosilicate (TEOS), 3-Aminopropyl-Triethoxysilane (APTES), glacial acetic acid, dichloromethane, methanol, acetone, Tetrahydrofuran (THF), $FeCl_3 \cdot 6H_2O$ were purchased from Tianjin Fuchen chemistry. Terephthalic aldehyde, nafoxidine, pyrrole, 4,4'-Diformyl-l,l'-biphenyl, were purchased from Energy chemical. All reagents used in this work were Analytical Regents (AR) and used without any further purification except pyrrole was distilled under reduced pressure.

B. Synthesis

1) Synthesis of SiO_2 nanoparticles

Monodispersed SiO_2 nanoparticles were synthesized according to the typical Stöber method reported before [8]. TEOS (6 mL) was added to a mixture of ethanol (74 mL),

deionized water (10 mL) and ammonia solution (3.14 mL). The silica colloidal solution was vigorously stirred for further 1 h at 30 ℃. The SiO_2 nanoparticles were collected by centrifugation at 10000 rpm for 15 min, washed and dried under vacuum.

2) Surface modification of SiO_2 nanoparticles

SiO_2 nanoparticles (2 g) were dispersed into ethanol (125 mL) under nitrogen atmosphere, and APTES (7.5 mL) was added dropwise. The reaction was kept at 60 ℃ for 24 h. The aminated SiO_2 nanoparticles were collected. Aminated SiO_2 nanoparticles (500 mg) were dispersed into ethanol (30 mL) under nitrogen atmosphere (named solution A). Terephthalic aldehyde (2 g) and nafoxidine (5 mL) were dispersed into ethanol (70 mL) under nitrogen atmosphere (named solution B). Solution A was added to solution B at 50 ℃ by peristaltic pump at a speed of 500 μL/min. The reaction was kept at 50 ℃ for 12 h. The aldehyde-coated SiO_2 nanoparticles were obtained by centrifugation, washed with dichloromethane until the supernatant transparent and finally dried under vacuum.

3) Synthesis of H-POP nanoparticles

A typical procedure for the post-treatment was carried out as follows. Aldehyde-coated SiO_2 nanoparticles (30 mg) were dispersed into glacial acetic acid (2 mL) under nitrogen atmosphere. Pyrrole/glacial acetic acid solution (3 mL, 0.005 g/mL) was added to the solution above and sonicate for 1 h. Then, $FeCl_3 \cdot 6H_2O$/glacial acetic acid solution (5 mL, 0.048 g/mL) was added. After that, 4,4'-Diformyl-l,l'-biphenyl (46.8 mg) /glacial acetic acid (5 mL) dispersion was added dropwise by a peristaltic pump at a speed of 100 μL/min. The reaction was kept at room temperature under nitrogen atmosphere and vigorous stirred in dark for 12 h. Then the mixture was transferred to a Teflon lined autoclave and kept under hydrothermal treatment for 72 h at 180 ℃. The obtained core-shell nanoparticles were filtered and thoroughly washed with methanol, acetone, THF, dichloromethane. Finally, H-POP nanoparticles were obtained by using 4% ammonium hydroxide aqueous solution etched SiO_2 nanoparticles cores. The mixture was transferred to a Teflon lined autoclave and kept under hydrothermal treatment for 18 h at 150 ℃. The yielding H-POP nanoparticles were collected by filtration, rinsed with ethanol and finally dried at room temperature.

C. Characterization

The nitrogen adsorption isotherm was measured on an Autosorb iQ-MP/XR adsorptometer, Quantachrome Instruments. The Power X-Ray Diffraction (PXRD) was performed by a Riguku smartlab diffractometer using Cu Kα radiation. Transmission Electron Microscopy (TEM) micrographs were recorded using a JEM-2100F with an acceleration voltage of 200 kV. Fourier-Transform Infrared Spectroscopy (FTIR) spectra were measured using a Bruker IFS66V fourier transform infrared spectrometer.

III. Results and Discussion

A. Modification of SiO_2 Template

The size is a critical parameter for the in vivo application. According to the Enhanced Permeability and Retention (EPR) effect, the nanoparticles smaller than 100 nm have higher permeability and retention comparing to bigger particles [9]. For the target size in the range of 50–100 nm, SiO_2 nanoparticles with the diameter of 40 nm was chosen as templates. For avoid the separation of the POPs and template, SiO_2 was modified with amino group and aldehyde group before use. The infrared spectrum of two types of amino group and following aldehyde group modified spheres is presented in Fig. 2(a). SiO_2-NH_2 revealed a strong absorption peak round around 3300 cm^{-1} and SiO_2-CHO had an obvious peak around 1700 cm^{-1} [10, 11]. These two peaks showed that the modified process for the SiO_2 spheres is successful.

B. Morphology and Thickness Controlling

Morphology controlling of the porphyrin POPs was performed by adding the modified SiO_2 templates to the synthesis system. The ratio of the monomers to the templates was adjusted to control the thickness of porphyrin POPs shell. The samples with ratios described in typical procedure together with double and triple ratio was noted as H-POP-1, H-POP-2, and H-POP-3.

The sample of H-POP-1was selected to exhibit the basic characterization. In Fig. 2(b), the Powder XRD analysis, the spectra revealed a broad peak at around 2θ = 24°, which indicate an amorphous nature of structure [12]. There is an additional small diffraction peak at 2θ = 7° comparing the bulk sample, suggest the ordered arrangement of the silica sphere templates. The result was further confirmed by TEM measurement. It proved that under acid environment and the exist of Fe^{3+}, pyrrole and 4'-Diformyl-l,l'-biphenyl took place an extended aromatic substitution reaction to form an amorphous framework.

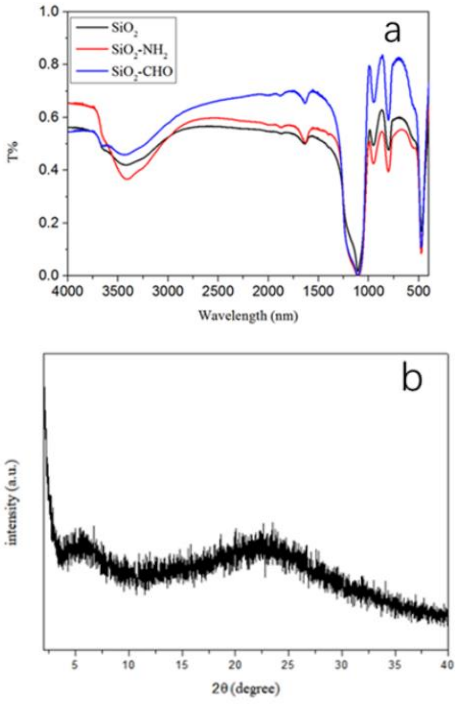

Fig. 2. (a) IR absorption spectra of modified Spheres. (b) XRD analysis of H-POP.

The adsorption isotherm of H-POP-1 in Fig. 3 showed a combine of Type I and Type IV isotherms [13]. At the low relative pressure, the gas adsorption went up dramatically, indicated the micropores in the structure. For the hysteresis

loop in the range of 0.42 and 0.95 of relative pressure, it always indicates mesoporous structure, which is defined as the pore widths between 2 and 50 nm by the International Union of Pure and Applied Chemistry (IUPAC) [14, 15]. In the bulk sample of porphyrin POPs, the additional mesoporous is not observed. This result indicated that the templates induced the hierarchical pore in the H-POP. The surface area of the H-POP was calculated with Brunauer-Emmett-Teller (BET) to be 549 m^2/g, which is little lower than the bulk sample.

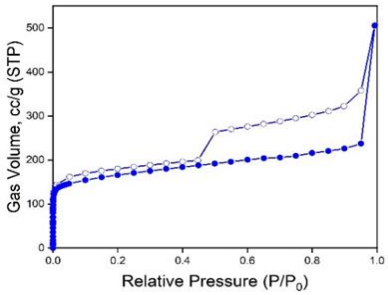

Fig. 3. The adsorption isotherm of H-POP.

At last, the TEM was employed to confirm the final morphology of the H-POPs. Fig. 4 showed that all three samples with the silica templates. In the TEM images, all the H-POPs indicated spherical morphology. The final size varied from 63 to 78 nm according to the monomer/template ratio. It is noteworthy that with the increase of monomer/template ratio, the aggregated level demonstrated an increasing trend. With the highest ratio, H-POP-3 showed the aggregation structure with a hollow structure.

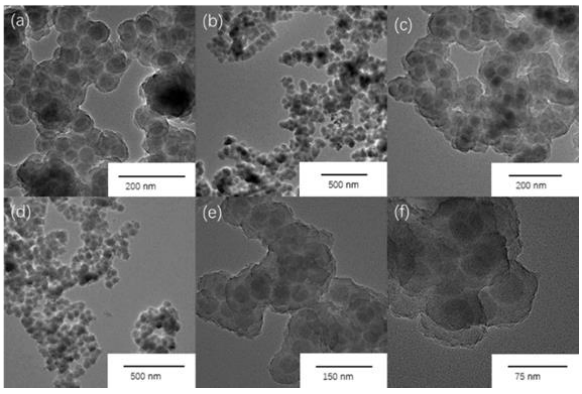

Fig. 4. TEM images of the (a)–(b) H-POP-1 and the (c)–(d) H-POP-2 and the (e)–(f) H-POP-3 with SiO_2 templates.

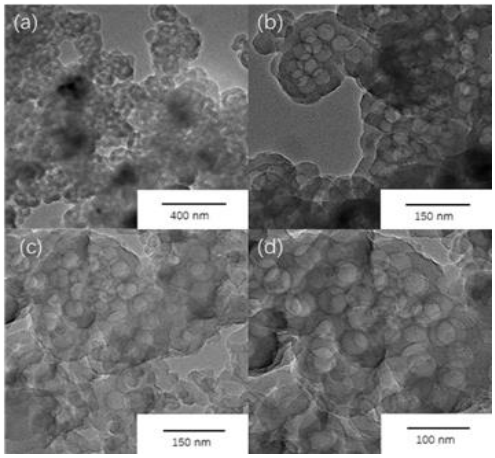

Fig. 5. TEM images of the (a), (c) H-POP-2 and the (b), (d) H-POP-3.

After the synthesis of H-POPs, samples were etched by aqueous ammonia in order to obtain hollow morphological structures. Fig. 5 indicated H-POP-2 and H-POP-3 samples with the templates etched.

IV. Conclusion

In conclusion, a morphological engineering of porphyrin POPs was performed by hard template method and the procedures were simple and affordable. Employed SiO_2 nanoparticle as the template, nano hollow porphyrin POPs were synthesized through a facile bottom-up approach by using extended aromatic substitution reaction of pyrrole with 4,4-diformyl-1,1'-biphenyl. The final size and shell thickness can be fine turned by the ratios of monomers and templates. By miniaturization porphyrin-POP to nanoscale, the water-dispersibility and cell permeability of H-POP will be improved. The series of H-POPs will serve as a strong candidate of multifunction platform for PDT PTT and chemotherapeutics.

Conflict of Interest

The author declares no conflict of interest.

Acknowledgment

The author thanks all those who helped me during the writing of this paper. My supervisor, Professor Zhao and seniors in the lab taught me laboratory skills and corrected the mistakes in this paper.

References

[1] A. Y. Rwei, W. Wang, and D. S. Kohane, "Photoresponsive nanoparticles for drug delivery," *Nano Today*, vol. 10, pp. 451–467, 2015.

[2] J. Tian, B. Huang, M. H. Nawaz, and W. Zhang, "Recent advances of multi-dimensional porphyrin-based functional materials in photodynamic therapy," *Coordination Chemistry Reviews*, vol. 420, pp. 1–20, 2020.

[3] Y. Kuang, K. Balakrishnan, V. Gandhi, and X. Peng, "Hydrogen peroxide inducible DNA cross-linking agents: Targeted anticancer prodrugs," *Journal of the American Chemical Society*, vol. 133, pp. 19278–19281, 2011.

[4] H. Maeda, J. Wu, T. Sawa, Y. Matsumura, and K. Hori, "Tumor vascular permeability and the EPR effect in macromolecular therapeutics: A review," *Journal of Controlled Release*, vol. 65, pp. 271–284, 2000.

[5] C. W. Kang, D. H. Lee, Y. J. Shin *et al.*, "Conjugated macro–microporous polymer films bearing tetraphenylethylenes for the enhanced sensing of nitrotoluenes," *Journal of Materials Chemistry A*, vol. 6, pp. 17312–17317, 2018.

[6] X. Zheng, L. Wang, Q. Pei, S. He, S. Liu, and Z. Xie, "Metal-organic Framework@Porous organic polymer nanocomposite for photodynamic therapy," *Chemistry of Materials*, vol. 29, pp. 2374–2381, 2017.

[7] K. M. Smith, "Development of porphyrin syntheses," *New Journal of Chemistry*, vol. 40, pp. 5644–5649, 2016.

[8] Y. J. Wong, L. Zhu, W. S. Teo, Y. W. Tan, Y. Yang, C. Wang, and H. Chen, "Revisiting the Stöber Method: Inhomogeneity in Silica Shells. *Journal of the American Chemical Society*, vol. 133, pp. 11422–11425, 2011.

[9] N. Alasvand, A. M. Urbanska, M. Rahmati *et al.*, "Chapter 13: Therapeutic nanoparticles for targeted delivery of Anticancer drugs," in *Multifunctional Systems for Combined Delivery, Biosensing and Diagnostics*, A. M. Grumezescu, Eds. Elsevier, 2017, pp. 245–259, 2017.

[10] R. Qu, M. Wang, C. Sun *et al.*, "Chemical modification of silica-gel with hydroxyl- or amino-terminated polyamine for adsorption of Au(III)," *Applied Surface Science*, vol. 255, pp. 3361–3370, 2008.

[11] E. Tiryaki, Y. B. Elalmış, B. K. İkizler, and S. Yücel, "Novel organic/inorganic hybrid nanoparticles as enzyme-triggered drug

delivery systems: Dextran and Dextran aldehyde coated silica aerogels," *Journal of Drug Delivery Science and Technology*, vol. 56, pp. 1–13, 2020.
[12] A. Modak, M. Nandi, J. Mondal, and A. Bhaumik, "Porphyrin based porous organic polymers: Novel synthetic strategy and exceptionally high CO_2 adsorption capacity," *Chemical Communications*, vol. 48, pp. 248–250, 2012.
[13] M. A. Al-Ghouti and D. A. Da'ana, "Guidelines for the use and interpretation of adsorption isotherm models: A review," *Journal of Hazardous Materials*, vol. 393, pp. 1–100, 2020.
[14] S. Das, P. Heasman, T. Ben, and S. Qiu, "Porous organic materials: strategic design and structure–function correlation," *Chemical Reviews*, vol. 117, pp. 1515–1563, 2017.
[15] C. G. V. Burgess, D. H. Everett, and S. Nuttall, "Adsorption hysteresis in porous materials," *Pure and Applied Chemistry*, vol. 61, pp. 1845–1852, 1989.